Cell

XMAP215 Is a Processive Microtubule Polymerase

Gary J. Brouhard,[1,5] Jeffrey H. Stear,[1,4,5] Tim L. Noetzel,[1] Jawdat Al-Bassam,[2] Kazuhisa Kinoshita,[3] Stephen C. Harrison,[2] Jonathon Howard,[1,*] and Anthony A. Hyman[1,*]
[1]Max Planck Institute of Molecular Cell Biology and Genetics, Dresden, Germany
[2]Department of Biological Chemistry and Molecular Pharmacology, Harvard Medical School, Boston, MA, USA
[3]Graduate School of Biostudies, Kyoto University, Kyoto, Japan
[4]Present address: Max Delbrück Center for Molecular Medicine, Berlin-Buch, Germany.
[5]These authors contributed equally to this work.
*Correspondence: howard@mpi-cbg.de (J.H.), hyman@mpi-cbg.de (A.A.H.)
DOI 10.1016/j.cell.2007.11.043

SUMMARY

Fast growth of microtubules is essential for rapid assembly of the microtubule cytoskeleton during cell proliferation and differentiation. XMAP215 belongs to a conserved family of proteins that promote microtubule growth. To determine how XMAP215 accelerates growth, we developed a single-molecule assay to visualize directly XMAP215-GFP interacting with dynamic microtubules. XMAP215 binds free tubulin in a 1:1 complex that interacts with the microtubule lattice and targets the ends by a diffusion-facilitated mechanism. XMAP215 persists at the plus end for many rounds of tubulin subunit addition in a form of "tip tracking." These results show that XMAP215 is a processive polymerase that directly catalyzes the addition of up to 25 tubulin dimers to the growing plus end. Under some circumstances XMAP215 can also catalyze the reverse reaction, namely microtubule shrinkage. The similarities between XMAP215 and formins, actin polymerases, suggest that processive tip tracking is a common mechanism for stimulating the growth of cytoskeletal polymers.

INTRODUCTION

Microtubules are long, slender filaments with which cellular structures such as the cytoskeleton, the mitotic spindle, and the axoneme are built. These structures are not static. Rather, they are broken down and rebuilt when a cell moves, changes shape, or progresses through the cell cycle. This remodeling is achieved by the disassembly and reassembly of microtubules and occurs primarily through the removal and addition of tubulin dimers at microtubule ends. Microtubule growth is fast. For example, in *Xenopus* oocytes (Gard and Kirschner, 1987b) and *C. elegans* embryos (Srayko et al., 2005) microtubules grow at rates of up to 40 $\mu m \cdot min^{-1}$. These high growth rates are necessary in order for the reassembly of the cytoskeleton to keep up with the progression of these rapidly dividing cells through the cell cycle. These in vivo growth rates are more than ten times higher than the corresponding rates for purified tubulin in vitro (Kinoshita et al., 2001) at cellular concentrations of tubulin (Hiller and Weber, 1978; Parsons and Salmon, 1997).

The accelerated microtubule growth rates in cells are mediated by members of the so-called Dis1/XMAP215 family of microtubule-associated proteins (Kinoshita et al., 2002). XMAP215 was first identified in *Xenopus laevis* egg extracts, where it was purified as a factor that increased the growth rate of microtubules in vitro 10-fold (Gard and Kirschner, 1987a). Genome sequencing has revealed homologs of XMAP215 in every eukaryotic organism investigated (Gard et al., 2004). Disruption of gene products in the Dis1/XMAP215 family results in the following phenotypes: (1) shorter meiotic or mitotic spindles in *Xenopus* egg extracts (Tournebize et al., 2000), *S. cerevisiae* (Severin et al., 2001), and *Drosophilia* S2 cells (Goshima et al., 2005); (2) disrupted interactions of microtubules with the cell cortex in *Dictyostelium* (Hestermann and Graf, 2004) and *Arabodopsis* (Whittington et al., 2001); and (3) disorganized spindle poles and aberrant spindle morphology in HeLa cells (Cassimeris and Morabito, 2004; Gergely et al., 2003), *S. pombe* (Garcia et al., 2001; Ohkura et al., 1988), and *C. elegans* (Matthews et al., 1998). These phenotypes are consistent with the observation that interfering with Dis1/XMAP215 decreases microtubule growth rates in *Xenopus* egg extracts (Tournebize et al., 2000), *C. elegans* embryos (Srayko et al., 2005), and *Drosophilia* S2 cells (Brittle and Ohkura, 2005). Several members of the Dis1/XMAP215 family localize to microtubule plus ends in vivo and in vitro (Hestermann and Graf, 2004; Nakaseko et al., 2001; van Breugel et al., 2003). This localization pattern is likely to be of general significance for the function of these proteins as the plus end is the primary site of microtubule growth in vivo.

How does XMAP215 increase the growth rate of microtubules? A hint about the mechanism comes from structural studies. Electron micrographs have shown both XMAP215 (Cassimeris et al., 2001) and Stu2p, the *S. cerevisiae* homolog (Al-Bassam et al., 2006), to be elongated and flexible molecules, with a contour length of ~60 nm. The most conserved features of the Dis1/XMAP215 family are the N-terminal TOG domains. The number of TOG domains varies from two to five, depending

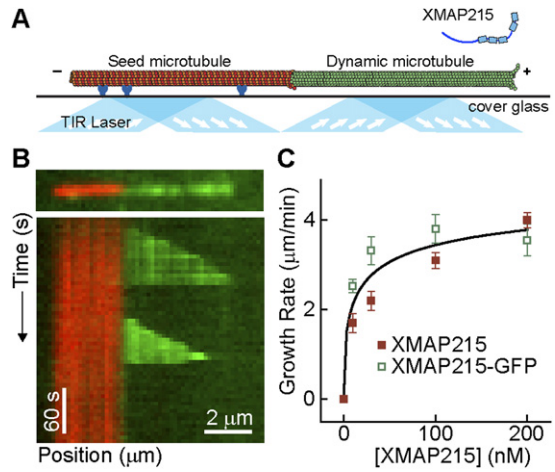

Figure 1. XMAP215 Promotes Microtubule Growth from the Plus End

(A) Schematic of the in vitro assay depicting a seed microtubule (red) immobilized above a cover glass surface by anti-rhodamine antibodies (dark blue). Two proteins are introduced, XMAP215 and tubulin (not shown). Polymerization occurs, resulting in the growth of a dynamic microtubule from the seed microtubule. Either the XMAP215 or the tubulin carries a fluorescent tag (see Experimental Procedures). Excitation by total internal reflection can allow the detection of single molecules in the evanescent field (see, e.g., Figures 2C and 2E). The schematic is not to scale.

(B) (Top) Still image of a seed microtubule (red) with a dynamic microtubule lattice growing from the plus end (green) in the presence of 100 nM XMAP215. (Bottom) Kymograph of the microtubule above, corresponding to Movie S1. Two periods of growth (rate = 3 $\mu m \cdot min^{-1}$) and two catastrophes are visible within the kymograph.

(C) Plot of microtubule growth rate versus XMAP215 concentration for XMAP215 and XMAP215-GFP. Data were fitted to the Hill equation (line drawn). Error bars represent the SEM ($n \geq 9$).

on the species; for example, Stu2p has two TOG domains, four in the Stu2p dimer (van Breugel et al., 2003), and XMAP215, a monomer (Cassimeris et al., 2001; Gard and Kirschner, 1987a), has five TOG domains. Each TOG domain contains six HEAT repeats that fold into a paddle-like structure (Al-Bassam et al., 2007). An individual TOG domain is sufficient to bind tubulin (Al-Bassam et al., 2007), leading to a high-affinity interaction between tubulin and Stu2p (Al-Bassam et al., 2006). TOGp, the human homolog, binds tubulin in vitro (Spittle et al., 2000), and XMAP215 coimmunoprecipitates with tubulin in *Xenopus* egg extracts (Niethammer et al., 2007). The binding of these proteins to tubulin dimers suggests that they bring tubulin from solution to the microtubule end. Acceleration of growth could result from rapid cycling onto and off the microtubule end or from multiple tubulins being brought at once. The high-affinity binding of tubulin has been proposed to account for the paradoxical finding that some of these family members can cause depolymerization in vitro (Al-Bassam et al., 2006; Shirasu-Hiza et al., 2003; van Breugel et al., 2003).

The prevailing model to explain the acceleration of microtubule growth by XMAP215 is that it acts as a "tubulin shuttle" that brings several tubulin dimers to the microtubule end (Gard and Kirschner, 1987a; Kerssemakers et al., 2006; Slep and Vale, 2007; Vasquez et al., 1994). Recent evidence for this model has come from high-resolution optical trapping experiments in which discrete length changes of up to 60 nm, the length of 7–8 tubulin dimers, were observed during microtubule growth (Kerssemakers et al., 2006), and from turbidity measurements in which artificially tetramerized TOG domains promoted microtubule nucleation in vitro (Slep and Vale, 2007). The model is not consistent, however, with experiments on other members of the Dis1/XMAP215 family. For example, Stu2p binds only one tubulin dimer in solution (Al-Bassam et al., 2006). Moreover, the observation that XMAP215, under certain conditions in vitro, can depolymerize microtubules has led to an alternative model in which XMAP215 acts as an antipause factor (Shirasu-Hiza et al., 2003).

To distinguish among the different possible ways that XMAP215 might promote microtubule growth, we developed an assay to visualize single XMAP215 molecules during microtubule polymerization. We demonstrate that XMAP215 does not, in fact, act as a tubulin shuttle. Rather, XMAP215 acts as a processive polymerizing enzyme or polymerase: XMAP215 forms a 1:1 complex with tubulin and resides for long periods at microtubule plus ends, where it catalyzes repeated rounds of addition of tubulin into the microtubule polymer.

RESULTS

XMAP215 Promotes Microtubule Growth

To determine how XMAP215 increases the growth rate of microtubules, we developed a fluorescence microscopy assay to visualize microtubule growth. To overcome the background fluorescence from free tubulin, which obscures the growing microtubule, we used total-internal-reflection fluorescence microscopy (TIRF), in which the excitation light is restricted to a narrow region near the cover glass. To keep the microtubule within the excitation field, we used antibodies specific to rhodamine to adhere GMPCPP-stabilized, rhodamine-labeled microtubule seeds to the cover glass surface (see Figure 1A and Experimental Procedures). Microtubules grew by extension from the microtubule seeds.

When a mixture of 4.5 μM unlabeled tubulin and 0.5 μM Alexa Fluor 488-labeled tubulin (Alexa-tubulin) was perfused into the chamber in the presence of 100 nM XMAP215 and 1 mM GTP, microtubules were observed to grow from the GMPCPP seeds. Polarity-marked microtubules were used to confirm this growth occurred from the plus end, as expected (see Supplemental Data, section 2.1). At this tubulin concentration, no microtubule growth was observed either at the minus ends or in the absence of XMAP215. Figure 1B shows a kymograph of a microtubule plus end undergoing two rounds of growth and shrinkage (see also Movie S1). XMAP215 promoted microtubule growth in a concentration-dependent manner, as shown in Figure 1C. These XMAP215-stimulated microtubule growth rates are in agreement with published values (Gard and Kirschner, 1987a; Kinoshita et al., 2001; Vasquez et al., 1994). We measured microtubule growth rates as a function of tubulin concentration, and at 200 nM XMAP215 the growth rates correspond to a second-order association rate constant of tubulin to the microtubule end of $19.8 \pm 2.6\ \mu M^{-1} \cdot s^{-1}$ (mean ± SEM, n = 9, see Supplemental Data, section 2.2). This association rate constant is 5- to 10-fold higher than the rate constant measured for the growth

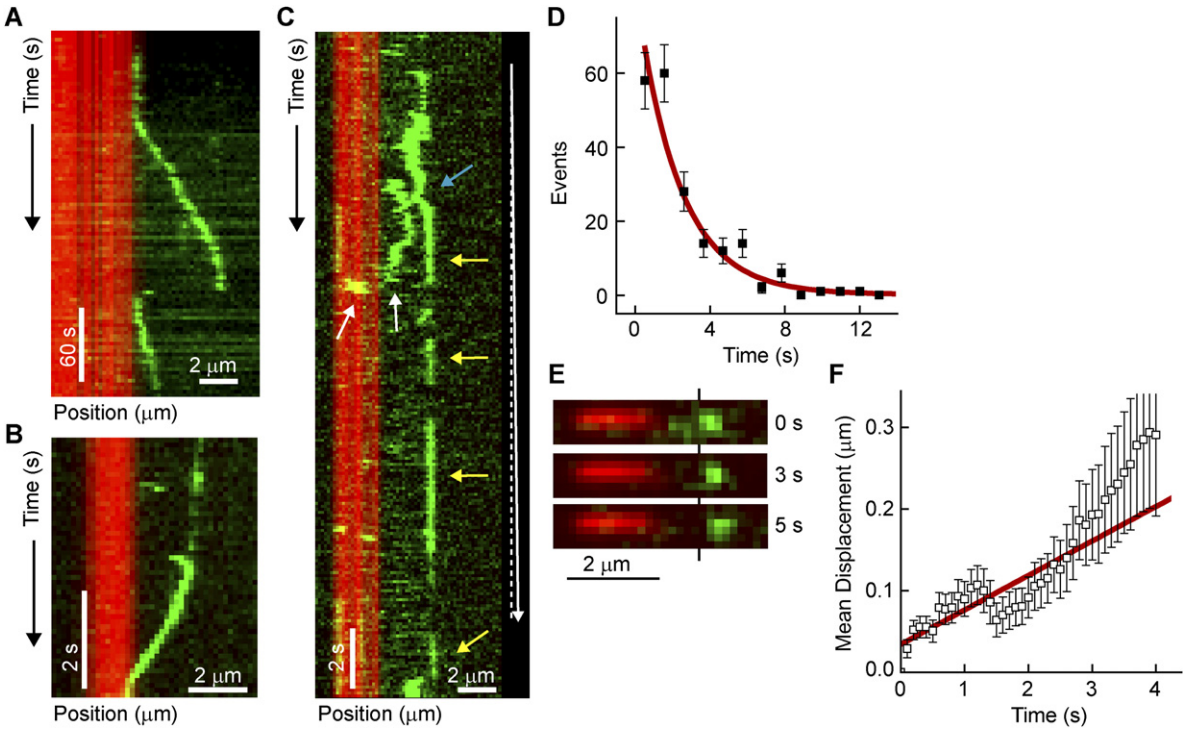

Figure 2. XMAP215 Tracks with Dynamic Microtubule Ends

(A) Kymograph of XMAP215-GFP molecules (50 nM) associated with a plus end during growth by "tip tracking." The seed microtubule is shown in red and XMAP215-GFP is shown in green. Taken from time-lapse microscopy.

(B) Kymograph depicting XMAP215-GFP (green) associated with the plus end of a dynamic lattice during shrinkage following a catastrophe.

(C) Kymograph from a spike experiment, showing single XMAP215-GFP molecules (green) associating with a dynamic plus end (yellow arrows) and diffusing on freshly polymerized lattice (white arrows). Taken from streaming video. The white arrow at right illustrates the outward displacement of the XMAP215-GFP molecules.

(D) Histogram of durations of single XMAP215-GFP end residence events. An exponential curve fit (red line) corrected for photobleaching gives a mean end-residence time, $\langle t_{END} \rangle$, of 3.8 ± 0.7 s.

(E) Still series of a single XMAP215-GFP molecule moving with the microtubule plus end during growth.

(F) Plot of the mean displacement of XMAP215-GFP end-residence events versus time. Data were fitted to a line, the slope of which gives the velocity of outward displacement. Error bars represent the SEM (n = 198).

of tubulin alone in our assay (see Supplemental Data, section 2.2) and reported in the literature (Howard, 2001).

XMAP215 Binds to Growing and Shrinking Plus Ends

In order to investigate how XMAP215 stimulates the association rate of tubulin, we looked at the interaction of XMAP215 with microtubules during microtubule growth. We visualized XMAP215 using a C-terminal GFP tag and TIRF microscopy; the microtubule seed is visualized by epifluorescence. The GFP-tagged XMAP215 had similar microtubule growth-promoting properties to the untagged protein (see Figure 1C).

At XMAP215-GFP concentrations between 50 and 200 nM, we observed distinct GFP foci at the microtubule plus end by time-lapse microscopy (see Figure 2A and Movie S2). These foci grew from the ends of the microtubules with an outward velocity that correlated with the previously measured microtubule growth rates for the given concentration of XMAP215 and tubulin (see above). Therefore, we conclude that these foci represent XMAP215-GFP molecules at the growing end of the microtubules, indicating that XMAP215 molecules "tip track" with the plus end of microtubules. In Figure 2A, we estimate there are ~10 XMAP215 molecules at the end based on fluorescence intensity. We note with interest that XMAP215-GFP also remained associated with the plus ends of microtubules during shrinkage (Figure 2B), often traveling >4 μm before encountering the microtubule seed. In addition, XMAP215-GFP molecules on the lattice were "picked up" by the shrinking plus end, causing an increase in GFP signal at the microtubule end as the shrinkage continued (data not shown). This phenomenon is similar to that observed for the Dam1 complex on shrinking microtubules (Westermann et al., 2006). Thus, XMAP215-GFP binds to both growing and shrinking plus ends of dynamic microtubules.

The presence of multiple XMAP215-GFP molecules at the microtubule end and the use of time-lapse microscopy prevented us from observing the behavior of individual XMAP215-GFP molecules. To follow individual XMAP215-GFP molecules during microtubule polymerization, we performed "spike" experiments in which <5 nM XMAP215-GFP was added to ~95 nM unlabeled XMAP215, and movies were recorded using continuous streaming video. Single molecules of XMAP215-GFP were observed

diffusing on the dynamic microtubule lattice and the microtubule seed (see Figure 2C, white arrows). The diffusion coefficient of this motion was D = 0.30 ± 0.01 $\mu m^2 \cdot s^{-1}$, and the mean residence time on the lattice was $\langle t \rangle$ = 2.45 ± 0.21 s (see Supplemental Data, section 3). In addition, XMAP215 molecules were observed to diffuse to and then bind to the microtubule ends (see Figure 2C, blue arrow).

Further analysis of the spike experiments showed that single XMAP215-GFP molecules resided for extended periods at the growing microtubule end (see Figure 2C, yellow arrows, and Movie S3). After correction for photobleaching, the mean residence time of XMAP215 at the microtubule end was $\langle t_{END} \rangle$ = 3.8 ± 0.7 s (Figure 2D, n = 198 molecules, see Supplemental Data, section 3). In these experimental conditions, no microtubule growth occurred in the absence of XMAP215; we can therefore attribute all tubulin dimer additions to XMAP215. During the 3.8 s residence time of individual XMAP215-GFP molecules, the microtubule grew by ~0.2 μm (for the measured growth rate of 3.0 $\mu m \cdot min^{-1}$ or 82 dimers$\cdot s^{-1}$), corresponding to ~330 tubulin dimers or ~25 tubulin dimers onto each of 13 protofilaments. Therefore, on average, the XMAP215-GFP molecules are present during the addition of at least 25 tubulin dimers if one XMAP215-GFP binds to each protofilament and greater numbers if fewer than 13 XMAP215s bind to the microtubule end at once.

XMAP215 Moves with the Growing Plus End

The results in the previous section show that on average XMAP215 resides at the growing plus end of the microtubule for a time during which the microtubule grows by ~0.2 μm. To see whether XMAP215 moved with the growing end during its residence time, we examined the single-molecule end events more closely. We observed single XMAP215 molecules moving away from the microtubule seed (Figure 2E), suggesting that XMAP215 tracks with the growing plus end. To test whether this tracking corresponded to the observed microtubule growth, we measured the outward displacement of the single molecules of XMAP215 at microtubule ends in the spike experiments. The mean displacement was 0.17 ± 0.1 μm (mean ± SEM, n = 198), which corresponds to ~21 tubulin dimer lengths. Furthermore, the mean velocity of outward displacement was 2.7 ± 0.25 $\mu m \cdot min^{-1}$ (Figure 2F), which is similar to the measured growth rate of microtubules in the presence of 100 nM XMAP215. Therefore, the outward displacements are consistent with single XMAP215 molecules tracking with the plus end of the microtubule during growth.

XMAP215 Binds Tubulin with 1:1 Stoichiometry

How does XMAP215 promote the addition of so many tubulin dimers during its interaction with the microtubule end? Previous work has shown that TOG domains can bind tubulin (Al-Bassam et al., 2007). Using size-exclusion chromatography, we confirmed that XMAP215, like the *S. cerevisiae* homolog Stu2p (Al-Bassam et al., 2006), binds tubulin (see Figures 3A and 3B and Supplemental Data, section 4.1). We analyzed the XMAP215:tubulin complex by negative stain electron microscopy and compared it with free XMAP215. As previously observed (Cassimeris et al., 2001), free XMAP215 is a thin rod with multiple flexible joints (Figure 3C). These joints are likely to be the disordered sequences between XMAP215's five ordered TOG domains; free Stu2p has a similar appearance (Al-Bassam et al., 2006). The elongated structure is consistent with our measurement of the sedimentation coefficient of XMAP215 (see Supplemental Data, section 4.2). When it binds tubulin XMAP215 forms well-ordered globular complexes with a diameter of approximately 10 nm (Figure 3D). That is, the jointed, monomeric XMAP215 rod closes up around a tubulin dimer, forming a complex similar to that seen with dimeric Stu2p and tubulin (Al-Bassam et al., 2006).

The formation of an XMAP215:tubulin complex suggests that XMAP215 could escort free tubulin to the end of a microtubule, thereby increasing the association rate of tubulin dimers to the end. If this idea were correct, our measurements of the end-residence time indicate that either (1) one XMAP215 molecule binds to multiple tubulins and brings them en masse to the end of the microtubule, or (2) XMAP215 executes multiple rounds of tubulin addition at the microtubule end. We have distinguished between these possibilities by examining the stoichiometry of the XMAP215-tubulin interaction. First, we used our size-exclusion chromatography to show that XMAP215 and tubulin dimers are in a 1:1 complex (see Supplemental Data, section 4.1). We observed that XMAP215:tubulin complexes do not change their elution profile at tubulin concentrations higher than those used in our polymerization assays, demonstrating that it is not possible to force more than one tubulin dimer into the complex. Using sedimentation equilibrium analytical ultracentrifugation, we measured a molecular mass of 220 ± 10 kDa for XMAP215 alone (see Supplemental Data, section 4.3), confirming that XMAP215, with a predicted molecular mass of 228 kDa, is a monomer (Cassimeris et al., 2001; Gard and Kirschner, 1987a). We measured a molecular mass of 320 ± 30 kDa for the XMAP215:tubulin complex. The difference between these masses is 100 ± 32 kDa, indicating that the complex contains a single tubulin dimer (predicted mass: ~110 kDa).

These biochemical findings make it unlikely that XMAP215 binds to multiple tubulin dimers in solution. It remains possible, however, that XMAP215 binds multiple tubulin dimers when interacting with the microtubule lattice. We therefore used TIRF microscopy to determine whether XMAP215 binds to tubulin on the microtubule lattice and, if so, to measure the stoichiometry. GMPCPP-stabilized, rhodamine-labeled microtubules were adhered to the surface of a flow cell and incubated with 100 nM Alexa-tubulin. We could detect an association between Alexa-tubulin and the microtubules only in the presence of XMAP215 (unlabeled). At nanomolar concentrations of XMAP215, discrete foci of Alexa-tubulin were present along the microtubule (see Figure 4B). These tubulin foci moved randomly on the microtubule lattice in a manner comparable to the diffusive movement of XMAP215 alone (see Figure 4A). Like XMAP215-GFP, these particles targeted to the plus ends of microtubules. The diffusion coefficient and mean residence time of Alexa-tubulin were similar to those of XMAP215-GFP alone (see Figures 4C and 4D). The lattice interactions of XMAP215-GFP and the XMAP215:Alexa-tubulin complex were both dependent on the C terminus of tubulin, known as the "E-hook" (see Supplemental Data, section 5), suggesting an electrostatic interaction (Helenius et al., 2006). We

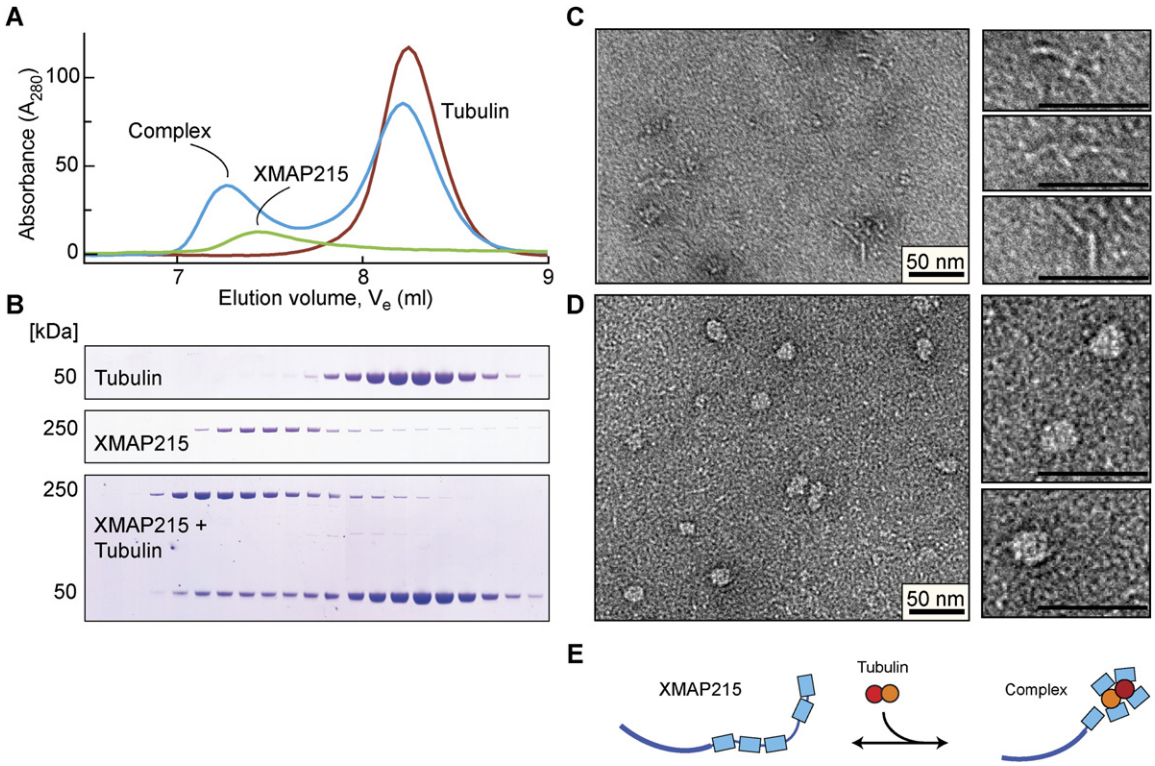

Figure 3. XMAP215 Forms a Complex with Tubulin

(A) Plot of A_{280} absorbance against elution volume from the size-exclusion chromatography experiments. Three traces are shown: tubulin alone (red), XMAP215 alone (green), and a complex of XMAP215 + one tubulin dimer (blue).

(B) Intensity scan of an SDS-PAGE gel taken from the above experiment. Lanes correspond to samples selected from the elution profile.

(C and D) Electron micrographs of negatively stained complexes of XMAP215 and tubulin. The panels on the right are at 2× magnification. Scale bars 50 nm. (C) shows the XMAP215 monomer. (D) shows the XMAP215:tubulin complex. The XMAP215:tubulin complex has a sedimentation coefficient indicative of an elongated molecule, indicating that the C terminus of XMAP215 may extend from the complex. Hints of the C-terminal extension are evident.

(E) Schematic showing XMAP215 with five TOG domains enclosing a single tubulin dimer to form a 1:1 complex. TOG domains are represented by light-blue boxes. The contour lengths of XMAP215 and the tubulin dimer are approximately to scale. The arrangement of the TOG domains in the complex with tubulin is not known.

measured the amount of labeled tubulin in each complex by comparing the average fluorescence intensity of the tubulin foci on the lattice with the intensity of tubulin dimers bound to the glass surface. The fluorescence results show a 1:1 stoichiometry of XMAP215 and tubulin on the microtubule lattice (I = 1713 ± 1002 A.U. for XMAP215:Alexa-tubulin, mean ± SD, n = 962; I = 1542 ± 761 A.U. for surface Alexa-tubulin, mean ± SD, n = 2197, see Supplemental Data, section 4.4). Thus, we conclude that XMAP215 does not bind to multiple tubulin dimers even when interacting with the microtubule lattice in the polymerization buffer. Our conclusion appears to contradict an earlier report that multiple tubulins can bind to XMAP215 (Cassimeris et al., 2001); however, the earlier experiments were performed in a very low ionic strength buffer, whereas our single-molecule experiments were performed in the same buffer conditions as our polymerization experiments.

XMAP215 Depolymerizes GMPCPP Microtubules in a Reversal of the Growth Reaction

An important consideration for the mechanism is whether growth stimulation by XMAP215 requires an energy source. Even though XMAP215 does not contain ATPase or GTPase domains, it could couple to the GTPase activity of tubulin. We have ruled out a requirement for the GTPase activity of tubulin by observing that XMAP215 stimulated the growth of tubulin in the presence of the slowly hydrolysable analog GMPCPP. The microtubule growth rate in 0.5 μM GMPCPP tubulin was 0.3 ± 0.15 $\mu m \cdot min^{-1}$ (8.8 ± 4.4 $dimers \cdot s^{-1}$) at 20 nM XMAP215 (mean ± SD, n = 54, see Supplemental Data, section 6), compared to 0.07 ± 0.02 $\mu m \cdot min^{-1}$ (2.0 ± 0.63 $dimers \cdot s^{-1}$) in the absence of XMAP215 (mean ± SD, n = 40). Thus, GTP hydrolysis is not required for XMAP215 to promote microtubule growth.

The absence of an energy requirement suggests that XMAP215 may act simply as a catalyst that accelerates growth by stabilizing an intermediate state in the reaction step at which the incoming tubulin dimer is incorporated into the lattice. We might then expect that in the absence of tubulin, XMAP215 should act in reverse; that is, it should remove tubulin dimers from the microtubule end, as has been observed (Shirasu-Hiza et al., 2003; see Introduction). To test for reversibility, we used a constant XMAP215 concentration of 100 nM while varying the free GTP-tubulin concentration from 0 to 5 μM (Movie S4).

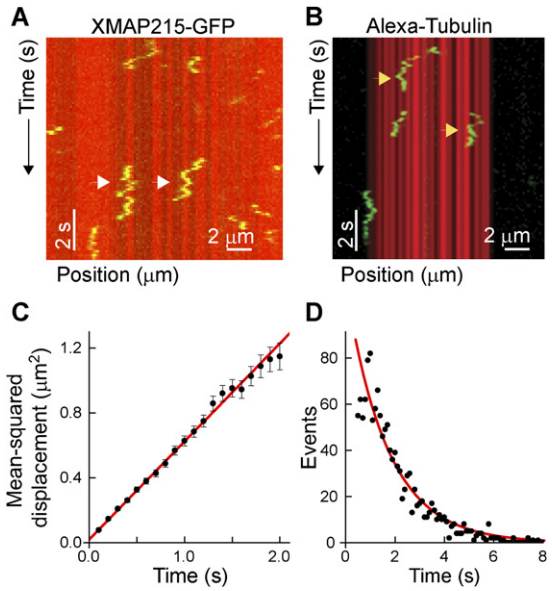

Figure 4. XMAP215 Targets One Tubulin to the Microtubule End by Lattice Diffusion

(A) Kymograph depicting the diffusion of XMAP215-GFP alone on a GMPCPP microtubule (white arrows).

(B) Kymograph depicting the XMAP215:tubulin complex diffusing on the microtubule (yellow arrows). Note the similarity to (A).

(C) Plot of mean-squared displacement for XMAP215-GFP against the time interval over which it was measured. A linear curve fit to the data yields a diffusion coefficient, D, of $0.3 \pm 0.01\ \mu m^2 \cdot s^{-1}$. Error bars are the SEM of the squared displacement values (n = 1383).

(D) Histogram of durations of XMAP215-GFP microtubule interactions. An exponential curve fit, corrected for photobleaching, yields a mean lifetime of the interactions, $\langle t \rangle$ of 2.45 ± 0.21 s.

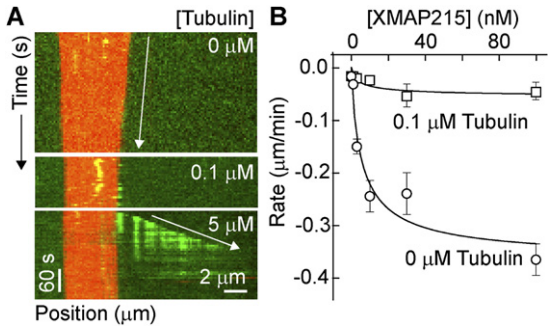

Figure 5. XMAP215 Catalyzes Both Growth and Shrinkage

(A) Kymograph of a single microtubule exposed to three tubulin concentrations at 100 nM XMAP215, corresponding to Movie S4. At 0 μM GTP-tubulin, the GMPCPP microtubule seed depolymerized (top). At 0.1 μM GTP-tubulin, the depolymerization was inhibited (middle), and at 5 μM GTP-tubulin, rapid microtubule growth occurred (bottom).

(B) Plot of the depolymerization rate against XMAP215 concentration at three different tubulin concentrations. Error bars represent the SEM ($n \geq 9$). The data were fitted to the Hill equation (line plotted). At 0.1 μM GTP-tubulin, depolymerization was inhibited.

The kymograph in Figure 5A shows the results from a single microtubule: at 0 μM tubulin, depolymerization of the GMPCPP seed occurred (Figure 5A, top); by adding 0.1 μM GTP-tubulin, this depolymerization was inhibited (Figure 5A, middle); and at 5 μM GTP-tubulin, growth occurred (Figure 5A, bottom). Thus, the same microtubule can grow or shrink, depending on the free GTP-tubulin concentration. It is important to note that the concentration of tubulin in cells (~10 μM, Hiller and Weber, 1978) would always promote growth. Like polymerization, the depolymerization rate depended on the XMAP215 concentration, increasing the shrinkage rate of GMPCPP microtubules up to 10-fold (Figure 5B). These data argue that XMAP215-mediated depolymerization is indeed a reversal of the growth reaction and that XMAP215 increases the dissociation rate constant as well as the association rate constant.

DISCUSSION

Our results show that XMAP215 is a processive polymerase that catalyzes numerous rounds of tubulin subunit addition while at the microtubule end and argue against the tubulin shuttle model. Our definition of a processive polymerase is as follows: by polymerase, we mean an enzyme that catalyzes the addition of individual subunits to the end of a polymer; by processive, we mean that multiple rounds of subunit addition are catalyzed by a single enzyme. The arguments against the tubulin shuttle model and for a processive polymerase model are 3-fold. First, we have shown that XMAP215 binds tubulin with 1:1 stoichiometry, both in solution and on the microtubule lattice. Therefore, XMAP215 cannot accelerate microtubule growth by adding multiple tubulin dimers en masse. Second, the flux of XMAP215 to the microtubule end is not high enough to deliver sufficient tubulin to the end to account for the growth rate. For example, at a growth rate of 3 $\mu m \cdot min^{-1}$, the microtubule grows at 82 dimers$\cdot s^{-1}$, but the estimated arrival rate of XMAP215 at the end from our experiments is only ~8 s^{-1} (see Supplemental Discussion, section 7 and Helenius et al., 2006). And third, XMAP215 resides at the growing plus end for more than ten times longer than the time required to act as a tubulin shuttle. Specifically, during the 3.8 s average end residence time, ~330 dimers are added to the microtubule end or ~25 tubulin dimers to each protofilament. Thus, while it is possible that one tubulin dimer is added by the shuttle mechanism, our results show that many more tubulin dimers are added when XMAP215 resides at the end, and 25 tubulin subunits corresponds to the minimum processivity for XMAP215.

How does XMAP215 mediate multiple cycles of tubulin addition while localized at the microtubule end? Any model for how XMAP215 catalyzes microtubule growth must take into account the following four experimental findings. First, XMAP215 forms a 1:1 complex with tubulin in solution. The affinity of XMAP215 for soluble tubulin (dissociation constant ≤ 1 μM based on size exclusion chromatography experiments) is relatively high compared to its affinity for lattice-incorporated tubulin, where the measured diffusion coefficient indicates that XMAP215 steps between adjacent lattice tubulins at a rate exceeding 1000 s^{-1} (Helenius et al., 2006). Perhaps, XMAP215 forms a 1:1 complex by interacting with tubulin surfaces that are exposed in the free dimer but hidden after the dimer has been incorporated into

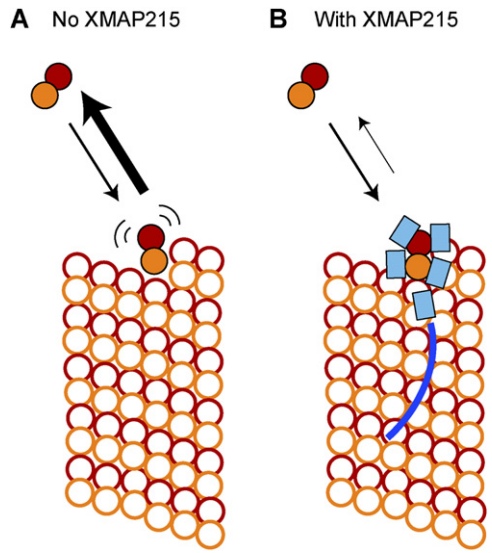

Figure 6. Model Diagram for Tubulin Polymerization by XMAP215

(A) Schematic of the plus end of a microtubule (hollow circles). A weakly attached tubulin is shown in full color. Tubulin dimers collide with the microtubule end in a diffusion-limited reaction (arrow pointing to microtubule), but these collision complexes are short lived, and the tubulin dimer often diffuses away (bold arrow pointing to solution).

(B) XMAP215 stabilizes the weakly attached tubulin dimer, so that a larger fraction incorporate into the microtubule (small arrow pointing to solution). Note that the collision complex forms at the same rate with or without XMAP215.

the microtubule. Second, XMAP215 prefers to bind to the microtubule plus end rather than to the middle of the microtubule lattice or to the minus end; it accelerates growth specifically at the plus end. XMAP215 therefore probably contacts exposed surface residues of tubulin that are present only at the plus end. Third, XMAP215 is present at the microtubule end for the addition of many tubulin dimers and moves outward with the growing plus end. Fourth, in the absence of free tubulin, XMAP215 depolymerizes microtubules. It seems that XMAP215 binds to the more weakly attached tubulin dimers at the end of the microtubule, pulls them from the lattice, and forms a 1:1 complex by a reversal of the polymerization mechanism.

These observations are brought together in the following model for how XMAP215 accelerates microtubule growth (Figure 6). The main concept of the model is that XMAP215 binds to and stabilizes a structural intermediate in the polymerization pathway. This intermediate state may correspond to a collision complex whose formation is very fast and diffusion limited. In the absence of XMAP215, the collision complex is very short lived, and tubulin often diffuses away instead of being incorporated into the microtubule (Figure 6A). XMAP215 stabilizes the intermediate state, so that there is a higher probability that the tubulin dimer will become strongly bound and ultimately incorporated in the lattice (Figure 6B). Our data indicate that XMAP215 increases the association rate constant of GTP-tubulin to the protofilament end from 0.3 $\mu M^{-1} \cdot s^{-1}$ to 1.5 $\mu M^{-1} \cdot s^{-1}$ (see Supplemental Discussion, section 7.1); thus, in the absence of XMAP215, microtubule growth is quite slow, and even in the presence of XMAP215, the association rate constant is below the diffusion-limited case (Northrup and Erickson, 1992).

This model explains why XMAP215 accelerates depolymerization. Because XMAP215 lowers the free energy of the intermediate state relative to the initial state (free tubulin and the microtubule end), it must also lower the free energy relative to the final state (strongly bound tubulin incorporated into the microtubule), implying that the reverse reaction, namely removal of tubulin from the end, must also be accelerated. Thus, we expect XMAP215 to accelerate microtubule shrinkage at low tubulin concentrations, as observed (Figure 5). This argument is formalized in a kinetic scheme in Supplemental Discussion, section 7.3. The scheme shows that, in the absence of an energy source, XMAP215 should increase the net association rate constant and the net dissociation rate constant to the same extent, with no change in the critical concentration. Our data in both GMPCPP-tubulin and GTP-tubulin are consistent with this expectation (see Supplemental Discussion, section 7.3.2). Thus, the stabilization of an intermediate state by XMAP215 accelerates the exchange of tubulin dimers into and out of the lattice. Although our specific kinetic model only considers a simple microtubule end structure, it should apply equally well to growth at the end of a closed tube (Mandelkow et al., 1991) or a sheet (Arnal et al., 2000; Chretien et al., 1995), both of which have been seen by electron microscopy, because the net energy difference associated with tubulin moving from solution into the lattice does not depend on the structure of the end.

The stabilization of a weakly attached dimer by XMAP215 could allow other tubulin dimers to attach naturally, at sites made favorable for tubulin association (i.e., XMAP215 creates new "snug" sites that allow microtubule growth). In this scenario, a single XMAP215-mediated stabilization could trigger multiple tubulin dimer additions. Such a mechanism alone is not consistent, however, with the longitudinal displacement of XMAP215 that we observe in the single-molecule experiments. Also, XMAP215 stays on the microtubule end for a time during which a large number of tubulin dimers are added (~25 rows of tubulin on average). Thus, XMAP215 does not trigger polymerization solely via a transient "kiss-and-run" interaction with the microtubule end. Instead, once XMAP215 has released its tubulin into the microtubule lattice, XMAP215 remains attached to the microtubule end, perhaps through an electrostatic interaction with the E-hooks. This interaction would allow it to quickly find a new binding site on the microtubule plus end. We do not exclude, however, a combination of XMAP215's processive outward displacement along with "filling in" of now-favorable binding sites.

Why does XMAP215 diffuse on the microtubule lattice? One possibility, mentioned in the previous paragraph, is that XMAP215 uses an electrostatic interaction with the E-hooks of lattice tubulins to remain bound to the end of the microtubule and polymerize processively. Such an increase in processivity mediated by the E-hooks has been previously observed for the directed motility of kinesin-1 (Thorn et al., 2000) and cytoplasmic dynein (Wang and Sheetz, 2000). Another possibility is that XMAP215 uses lattice diffusion to more rapidly target to the end initially, as has been shown for MCAK (Helenius et al., 2006). The diffusion of XMAP215 has much in common with MCAK, a microtubule depolymerase, although XMAP215 is not

a motor protein. Both proteins diffuse to their site of action, the end of a microtubule. A diffusion-facilitated search strategy enhances the rate of protein-protein association in various situations, with targeting of restriction enzymes to their restriction sites being a canonical example (Halford and Marko, 2004). Diffusive interactions with microtubules have recently been reported for the Dam1 complex (Westermann et al., 2006), Eg5 (Kwok et al., 2006), and myosin MyoVa (Ali et al., 2007), indicating that diffusion is a common mechanism of association for proteins with a microtubule surface. Diffusion of proteins is also common on the surfaces of intracellular membranes, and membrane diffusion of many enzymes is critical for their in vivo function. By analogy to membrane surfaces, we hypothesize that the microtubule surface may act as a "cellular compartment," on which the diffusive interactions of microtubule-associated proteins increase local concentration and orient the proteins correctly for productive intermolecular contact.

A processive polymerase model of XMAP215 may provide new insight into the regulation of XMAP215 by other cellular factors. For example, XMAP215 is positively stimulated by the protein XTACC3 (Kinoshita et al., 2005), and this enzyme pair is conserved in humans (Gergely et al., 2003), *C. elegans* (Srayko et al., 2003), *Drosophilia* (Lee et al., 2001), and *S. pombe* (Sato and Toda, 2007). One possibility is that XTACC3 promotes the catalytic activity of XMAP215 by increasing its processivity. XMAP215 is phosphorylated during M phase (Vasquez et al., 1999), and phosphorylation could alter numerous aspects of XMAP215 activity. For example, we predict that changes in the electrostatic character of XMAP215 would influence microtubule lattice binding through the E-hooks. It is also possible that phosphorylation could change the capacity of XMAP215 to bind free tubulin, to recognize the microtubule plus end, or to catalyze multiple rounds of tubulin subunit addition processively.

There are interesting similarities and differences between XMAP215 and formins, which catalyze the addition of multiple actin monomers to the end of growing actin filaments (Goode and Eck, 2007). Both "tip track," both increase the association rate of monomers by 5- to 10-fold, and both are processive (Kovar et al., 2006; Romero et al., 2004). The formins differ from XMAP215 in their very long end residence (>1000 s), but structurally, both bind their filament end and subunit simultaneously. For the formins, the relevant subunit is actin plus the adaptor molecule profilin, while XMAP215 acts on tubulin alone. The formins have FH1 domains, which bind profilin-actin (Romero et al., 2007), and FH2 domains, which bind the barbed end of the actin filament (Otomo et al., 2005). XMAP215 has TOG domains, which bind to the tubulin subunit. The regions responsible for end binding and lattice diffusion are not known, although the lattice diffusion of XMAP215 is likely to involve an electrostatic interaction with the E-hooks of tubulin. Thus, it appears that two processive polymerases have evolved to perform related functions for their respective filaments.

EXPERIMENTAL PROCEDURES

Tubulin and Microtubule Preparation

Porcine brain tubulin was purified as described (Ashford et al., 1998). Labeling of cycled tubulin with Alexa Fluor 488 or TAMRA (Invitrogen) was performed as described (Hyman et al., 1991). GMPCPP microtubules were grown as described (Hunter et al., 2003). Polarity-marked microtubules were made as described (Howard and Hyman, 1993). Subtilisin-digested microtubules were made as described (Helenius et al., 2006).

XMAP215 Purification

The coding region of XMAP215 was modified by addition of either a C-terminal His7 tag or a C-terminal enhanced green fluorescent protein (GFP) His7 tag and cloned into the pFastBac1 vector. From these constructs, we generated baculovirus (Bac-to-Bac system, Invitrogen) that was subsequently used to infect *Spodoptera frugiperda* cells. The purification of recombinant XMAP215 and XMAP215-GFP was based on previous protocols (Kinoshita et al., 2001) and is described in Supplemental Experimental Procedures, section 8.1. Protein concentration was determined using a Bradford assay (Bio-Rad Protein Assay) and absorbance at $\lambda = 280$ nm.

Imaging

The total-internal-reflection fluorescence imaging setup used for this work was previously described (Helenius et al., 2006). Images were collected with an Andor DV887 iXon camera on a Zeiss Axiovert 200 M microscope using a Zeiss 100X/1.45 α Plan-FLUAR objective. Standard filter sets were used to visualize GFP, Alexa Fluor 488, and TAMRA fluorescence. The integration time for continuous streaming video was 100 ms. The characterization of microtubule dynamics required time-lapse movies with intervals of 3–5 s between frames.

Assay Conditions

The preparation of silanized cover glasses and perfusion chambers was previously described (Helenius et al., 2006 and Supplemental Experimental Procedures, section 8.2). The assay protocol was modified to create conditions for microtubule growth. Reaction channels were first rinsed with BRB80: 80 mM PIPES at pH 6.9, 1 mM $MgCl_2$, and 1 mM EGTA. Reaction channels were incubated with 1% anti-rhodamine antibody (Invitrogen) in BRB80 for 5 min, followed by 1% pluronic F127 (Sigma) in BRB80 for 5 min, and finally rhodamine-labeled, GMPCPP stabilized microtubule seeds for 15 min. Channels were washed once with BRB80 and once with imaging buffer (IB): BRB80 supplemented with 75 mM KCl, 0.1 mg/ml BSA, 1% β-mercaptoethanol, 40 mM glucose, 40 μg/ml glucose oxidase, and 16 μg/ml catalase. The microtubule seeds were placed under the TIRF microscope for viewing. We used an objective heater (Zeiss) to warm the sample to 35°C. At this point, the assay can test multiple conditions, depending on what solution is perfused into the chamber of microtubule seeds.

(A) Observation of microtubule growth (Figures 1B and 1C) used IB plus 4.5 μM unlabeled tubulin, 0.5 μM Alexa Fluor 488 tubulin (Alexa-tubulin), unlabeled XMAP215 (0–200 nM), and GTP (1 mM). (B) Observation of XMAP215-GFP during microtubule growth (Figure 2) used IB plus 5 μM unlabeled tubulin, a mixture of unlabeled XMAP215 and XMAP215-GFP, and GTP (1 mM). See the figure legends for the concentrations of XMAP215 and XMAP215-GFP used in each experiment. (C) Observation of Alexa-tubulin interacting with XMAP215 (Figure 4B) used IB plus 100 nM unlabeled XMAP215, 5 nM Alexa Fluor 488 tubulin, and GTP (1 mM). (D) Observation of microtubule depolymerization (Figure 5B) used IB plus 100 nM unlabeled XMAP215. (E) Observation of the transition from shrinkage to growth (Figure 5A) used IB plus 100 nM XMAP215 and a series of 0 μM tubulin, 0.1 μM Alexa-tubulin, and 4.5 μM unlabeled tubulin, 0.5 μM Alexa-tubulin, and 1 mM GTP.

Image Analysis

Quantitative image analyses were performed as described (Helenius et al., 2006). Microtubule-length measurements were performed in Metamorph (Universal Imaging). Tracking of single molecules was performed in Motion Tracking by Y. Kalaidzidis (Transinsight GmbH). Trajectories for XMAP215-GFP molecules were exported from Motion Tracking to MATLAB (The MathWorks) for further analysis. All curve fitting was performed in OriginPro (OriginLab).

Size-Exclusion Chromatography and Gradient Sedimentation

Size-exclusion chromatography (Figures 3A and 3B) used a Tosoh TSKgelG5000PWXL column equilibrated in 25 mM TrisHCl, pH 7.5, 75 mM

NaCl, 1 mM $MgCl_2$, 1 mM EGTA, 0.1% Tween20, 1 mM DTT, and 0.2 mM GTP. The column was calibrated with standard proteins of known Stokes radii (GE Healthcare, see Supplemental Experimental Procedures, section 8.3). XMAP215 (5.7 μM) and tubulin (1.43 μM and 14.3 μM) were mixed with 1 mM GTP, incubated for 10 min on ice, and then injected onto the column. Control experiments were performed with each protein alone. The collected fractions (100 μl) were analyzed by SDS-PAGE, stained with Coomassie brilliant blue R250 (Merck), and scanned. The staining intensity in each fraction was compared to lanes containing known concentrations of tubulin or XMAP215 in order to estimate the concentration of proteins in each fraction. Sucrose-density gradients were performed and analyzed as described (Schurmann et al., 2001).

Sedimentation Equilibrium Analytical Ultracentrifugation

Sedimentation equilibrium experiments of full-length XMAP215 with and without tubulin were performed as described (Al-Bassam et al., 2006).

Electron Microscopy

Early fractions of size-exclusion chromatography experiments were evaluated using negative stain electron microscopy as described (Al-Bassam et al., 2006).

Supplemental Data

Supplemental Data include eight figures, one table, Supplemental Discussion, Supplemental Experimental Procedures, and four movies and can be found with this article online at http://www.cell.com/cgi/content/full/132/1/79/DC1/.

ACKNOWLEDGMENTS

We thank Y. Kalaidzidis and Transinsight GmbH for image analysis software; S. Diez and D. Drechsel for guidance; D. Cohen and E. Schäffer for the application of F-127; M. van Breugel for critical reading and early experiments with tubulin binding; S. Wolfson for editing; and members of the Howard and Hyman laboratories for discussions, reading, and feedback, especially J. Helenius, M. Srayko, and V. Varga. G.B. and J.S. were supported by the NIH NRSA program. J.A.B. was supported by the American Cancer Society. K.K. acknowledges a research grant from MEXT, Japan. S.C.H. is an Investigator in the Howard Hughes Medical Institute. This research was funded by the NIH (RO1 AR40593 to J.H.) and the Max Planck Society.

Received: June 29, 2007
Revised: September 17, 2007
Accepted: November 29, 2007
Published: January 10, 2008

REFERENCES

Al-Bassam, J., van Breugel, M., Harrison, S.C., and Hyman, A. (2006). Stu2p binds tubulin and undergoes an open-to-closed conformational change. J. Cell Biol. *172*, 1009–1022.

Al-Bassam, J., Larsen, N.A., Hyman, A.A., and Harrison, S.C. (2007). Crystal structure of a TOG domain: conserved features of XMAP215/Dis1-family TOG domains and implications for tubulin binding. Structure *15*, 355–362.

Ali, M.Y., Krementsova, E.B., Kennedy, G.G., Mahaffy, R., Pollard, T.D., Trybus, K.M., and Warshaw, D.M. (2007). Myosin Va maneuvers through actin intersections and diffuses along microtubules. Proc. Natl. Acad. Sci. USA *104*, 4332–4336.

Arnal, I., Karsenti, E., and Hyman, A.A. (2000). Structural transitions at microtubule ends correlate with their dynamic properties in Xenopus egg extracts. J. Cell Biol. *149*, 767–774.

Ashford, A.J., Anderson, S.S.L., and Hyman, A.A. (1998). Preparation of tubulin from bovine brain. In Cell Biology: A Laboratory Handbook (San Diego: Academic Press), pp. 205–212.

Brittle, A.L., and Ohkura, H. (2005). Mini spindles, the XMAP215 homologue, suppresses pausing of interphase microtubules in Drosophila. EMBO J. *24*, 1387–1396.

Cassimeris, L., and Morabito, J. (2004). TOGp, the human homolog of XMAP215/Dis1, is required for centrosome integrity, spindle pole organization, and bipolar spindle assembly. Mol. Biol. Cell *15*, 1580–1590.

Cassimeris, L., Gard, D., Tran, P.T., and Erickson, H.P. (2001). XMAP215 is a long thin molecule that does not increase microtubule stiffness. J. Cell Sci. *114*, 3025–3033.

Chretien, D., Fuller, S.D., and Karsenti, E. (1995). Structure of growing microtubule ends: two-dimensional sheets close into tubes at variable rates. J. Cell Biol. *129*, 1311–1328.

Garcia, M.A., Vardy, L., Koonrugsa, N., and Toda, T. (2001). Fission yeast ch-TOG/XMAP215 homologue Alp14 connects mitotic spindles with the kinetochore and is a component of the Mad2-dependent spindle checkpoint. EMBO J. *20*, 3389–3401.

Gard, D.L., Becker, B.E., and Josh Romney, S. (2004). MAPping the eukaryotic tree of life: structure, function, and evolution of the MAP215/Dis1 family of microtubule-associated proteins. Int. Rev. Cytol. *239*, 179–272.

Gard, D.L., and Kirschner, M.W. (1987a). A microtubule-associated protein from Xenopus eggs that specifically promotes assembly at the plus-end. J. Cell Biol. *105*, 2203–2215.

Gard, D.L., and Kirschner, M.W. (1987b). Microtubule assembly in cytoplasmic extracts of Xenopus oocytes and eggs. J. Cell Biol. *105*, 2191–2201.

Gergely, F., Draviam, V.M., and Raff, J.W. (2003). The ch-TOG/XMAP215 protein is essential for spindle pole organization in human somatic cells. Genes Dev. *17*, 336–341.

Goode, B.L., and Eck, M.J. (2007). Mechanism and function of formins in control of actin assembly. Annu. Rev. Biochem. *76*, 593–627.

Goshima, G., Wollman, R., Stuurman, N., Scholey, J.M., and Vale, R.D. (2005). Length control of the metaphase spindle. Curr. Biol. *15*, 1979–1988.

Halford, S.E., and Marko, J.F. (2004). How do site-specific DNA-binding proteins find their targets? Nucleic Acids Res. *32*, 3040–3052.

Helenius, J., Brouhard, G., Kalaidzidis, Y., Diez, S., and Howard, J. (2006). The depolymerizing kinesin MCAK uses lattice diffusion to rapidly target microtubule ends. Nature *441*, 115–119.

Hestermann, A., and Graf, R. (2004). The XMAP215-family protein DdCP224 is required for cortical interactions of microtubules. BMC Cell Biol. *5*, 24.

Hiller, G., and Weber, K. (1978). Radioimmunoassay for tubulin - quantitative comparison of tubulin content of different established tissue-culture cells and tissues. Cell *14*, 795–804.

Howard, J. (2001). Mechanics of Motor Proteins and the Cytoskeleton (Sunderland, MA: Sinauer Associates, Publishers).

Howard, J., and Hyman, A.A. (1993). Preparation of marked microtubules for the assay of the polarity of microtubule-based motors by fluorescence microscopy. Methods Cell Biol. *39*, 105–113.

Hunter, A.W., Caplow, M., Coy, D.L., Hancock, W.O., Diez, S., Wordeman, L., and Howard, J. (2003). The kinesin-related protein MCAK is a microtubule depolymerase that forms an ATP-hydrolyzing complex at microtubule ends. Mol. Cell *11*, 445–457.

Hyman, A., Drechsel, D., Kellogg, D., Salser, S., Sawin, K., Steffen, P., Wordeman, L., and Mitchison, T. (1991). Preparation of modified tubulins. Methods Enzymol. *196*, 478–485.

Kerssemakers, J.W., Munteanu, E.L., Laan, L., Noetzel, T.L., Janson, M.E., and Dogterom, M. (2006). Assembly dynamics of microtubules at molecular resolution. Nature *442*, 709–712.

Kinoshita, K., Arnal, I., Desai, A., Drechsel, D.N., and Hyman, A.A. (2001). Reconstitution of physiological microtubule dynamics using purified components. Science *294*, 1340–1343.

Kinoshita, K., Habermann, B., and Hyman, A.A. (2002). XMAP215: a key component of the dynamic microtubule cytoskeleton. Trends Cell Biol. *12*, 267–273.

Kinoshita, K., Noetzel, T.L., Pelletier, L., Mechtler, K., Drechsel, D.N., Schwager, A., Lee, M., Raff, J.W., and Hyman, A.A. (2005). Aurora A

phosphorylation of TACC3/maskin is required for centrosome-dependent microtubule assembly in mitosis. J. Cell Biol. *170*, 1047–1055.

Kovar, D.R., Harris, E.S., Mahaffy, R., Higgs, H.N., and Pollard, T.D. (2006). Control of the assembly of ATP- and ADP-actin by formins and profilin. Cell *124*, 423–435.

Kwok, B.H., Kapitein, L.C., Kim, J.H., Peterman, E.J., Schmidt, C.F., and Kapoor, T.M. (2006). Allosteric inhibition of kinesin-5 modulates its processive directional motility. Nat. Chem. Biol. *2*, 480–485.

Lee, M.J., Gergely, F., Jeffers, K., Peak-Chew, S.Y., and Raff, J.W. (2001). Msps/XMAP215 interacts with the centrosomal protein D-TACC to regulate microtubule behaviour. Nat. Cell Biol. *3*, 643–649.

Mandelkow, E.M., Mandelkow, E., and Milligan, R.A. (1991). Microtubule dynamics and microtubule caps: a time-resolved cryo-electron microscopy study. J. Cell Biol. *114*, 977–991.

Matthews, L.R., Carter, P., Thierry-Mieg, D., and Kemphues, K. (1998). ZYG-9, a Caenorhabditis elegans protein required for microtubule organization and function, is a component of meiotic and mitotic spindle poles. J. Cell Biol. *141*, 1159–1168.

Nakaseko, Y., Goshima, G., Morishita, J., and Yanagida, M. (2001). M phase-specific kinetochore proteins in fission yeast: Microtubule-associating Dis1 and Mtc1 display rapid separation and segregation during anaphase. Curr. Biol. *11*, 537–549.

Niethammer, P., Kronja, I., Kandels-Lewis, S., Rybina, S., Bastiaens, P., and Karsenti, E. (2007). Discrete states of a protein interaction network govern interphase and mitotic microtubule dynamics. PLoS Biol. *5*, 190–202.

Northrup, S.H., and Erickson, H.P. (1992). Kinetics of protein protein association explained by Brownian dynamics computer-simulation. Proc. Natl. Acad. Sci. USA *89*, 3338–3342.

Ohkura, H., Adachi, Y., Kinoshita, N., Niwa, O., Toda, T., and Yanagida, M. (1988). Cold-sensitive and caffeine-supersensitive mutants of the Schizosaccharomyces-pombe dis genes implicated in sister chromatid separation during mitosis. EMBO J. *7*, 1465–1473.

Otomo, T., Tomchick, D.R., Otomo, C., Panchal, S.C., Machius, M., and Rosen, M.K. (2005). Structural basis of actin filament nucleation and processive capping by a formin homology 2 domain. Nature *433*, 488–494.

Parsons, S.F., and Salmon, E.D. (1997). Microtubule assembly in clarified Xenopus egg extracts. Cell Motil. Cytoskeleton *36*, 1–11.

Romero, S., Didry, D., Larquet, E., Boisset, N., Pantaloni, D., and Carlier, M.F. (2007). How ATP hydrolysis controls filament assembly from profilin-actin: implication for formin processivity. J. Biol. Chem. *282*, 8435–8445.

Romero, S., Le Clainche, C., Didry, D., Egile, C., Pantaloni, D., and Carlier, M.F. (2004). Formin is a processive motor that requires profilin to accelerate actin assembly and associated ATP hydrolysis. Cell *119*, 419–429.

Sato, M., and Toda, T. (2007). Alp7/TACC is a crucial target in Ran-GTPase-dependent spindle formation in fission yeast. Nature *447*, 334–337.

Schurmann, G., Haspel, J., Grumet, M., and Erickson, H.P. (2001). Cell adhesion molecule L1 in folded (horseshoe) and extended conformations. Mol. Biol. Cell *12*, 1765–1773.

Severin, F., Habermann, B., Huffaker, T., and Hyman, T. (2001). Stu2 promotes mitotic spindle elongation in anaphase. J. Cell Biol. *153*, 435–442.

Shirasu-Hiza, M., Coughlin, P., and Mitchison, T. (2003). Identification of XMAP215 as a microtubule-destabilizing factor in Xenopus egg extract by biochemical purification. J. Cell Biol. *161*, 349–358.

Slep, K.C., and Vale, R.D. (2007). Structural basis of microtubule plus end tracking by XMAP215, CLIP-170, and EB1. Mol. Cell *27*, 976–991.

Spittle, C., Charrasse, S., Larroque, C., and Cassimeris, L. (2000). The interaction of TOGp with microtubules and tubulin. J. Biol. Chem. *275*, 20748–20753.

Srayko, M., Kaya, A., Stamford, J., and Hyman, A.A. (2005). Identification and characterization of factors required for microtubule growth and nucleation in the early C. elegans embryo. Dev. Cell *9*, 223–236.

Srayko, M., Quintin, S., Schwager, A., and Hyman, A.A. (2003). Caenorhabditis elegans TAC-1 and ZYG-9 form a complex that is essential for long astral and spindle microtubules. Curr. Biol. *13*, 1506–1511.

Thorn, K.S., Ubersax, J.A., and Vale, R.D. (2000). Engineering the processive run length of the kinesin motor. J. Cell Biol. *151*, 1093–1100.

Tournebize, R., Popov, A., Kinoshita, K., Ashford, A.J., Rybina, S., Pozniakovsky, A., Mayer, T.U., Walczak, C.E., Karsenti, E., and Hyman, A.A. (2000). Control of microtubule dynamics by the antagonistic activities of XMAP215 and XKCM1 in Xenopus egg extracts. Nat. Cell Biol. *2*, 13–19.

van Breugel, M., Drechsel, D., and Hyman, A. (2003). Stu2p, the budding yeast member of the conserved Dis1/XMAP215 family of microtubule-associated proteins is a plus end-binding microtubule destabilizer. J. Cell Biol. *161*, 359–369.

Vasquez, R.J., Gard, D.L., and Cassimeris, L. (1994). XMAP from Xenopus eggs promotes rapid plus end assembly of microtubules and rapid microtubule polymer turnover. J. Cell Biol. *127*, 985–993.

Vasquez, R.J., Gard, D.L., and Cassimeris, L. (1999). Phosphorylation by CDK1 regulates XMAP215 function in vitro. Cell Motil. Cytoskeleton *43*, 310–321.

Wang, Z.H., and Sheetz, M.P. (2000). The C-terminus of tubulin increases cytoplasmic dynein and kinesin processivity. Biophys. J. *78*, 1955–1964.

Westermann, S., Wang, H.W., Avila-Sakar, A., Drubin, D.G., Nogales, E., and Barnes, G. (2006). The Dam1 kinetochore ring complex moves processively on depolymerizing microtubule ends. Nature *440*, 565–569.

Whittington, A.T., Vugrek, O., Wei, K.J., Hasenbein, N.G., Sugimoto, K., Rashbrooke, M.C., and Wasteneys, G.O. (2001). MOR1 is essential for organizing cortical microtubules in plants. Nature *411*, 610–613.